Talanta 127 (2014) 152–162

Contents lists available at ScienceDirect

Talanta

journal homepage: www.elsevier.com/locate/talanta

Characterization of TATP gas phase product ion chemistry via isotope labeling experiments using ion mobility spectrometry interfaced with a triple quadrupole mass spectrometer

Jill Tomlinson-Phillips [a], Alfred Wooten [b], Joseph Kozole [a,c], James Deline [e], Pamela Beresford [d], Jason Stairs [e,*]

[a] ORISE Fellow at the U.S. Department of Homeland Security, Science & Technology Directorate, Transportation Security Laboratory, USA
[b] Battelle Memorial Institute, 2900 Fire Rd, Suite 201, Egg Harbor Township, NJ 08234, USA
[c] DuPont Central Research and Development, Experimental Station, Wilmington, DE, USA
[d] Global Systems Technologies, 2511 Fire Rd, Egg Harbor Township, NJ 08234, USA
[e] U.S. Department of Homeland Security, Science & Technology Directorate, Transportation Security Laboratory, Atlantic City International Airport, NJ 08405, USA

ARTICLE INFO

Article history:
Received 20 December 2013
Received in revised form
14 March 2014
Accepted 17 March 2014
Available online 2 April 2014

Keywords:
Explosives detection
Isotope labeling
Product ion
Molecular formula
Explosives
TATP
Ion mobility spectrometry (IMS)
Mass spectrometry (MS)
Ion chemistry

ABSTRACT

Identification of the fragment ion species associated with the ion reaction mechanism of triacetone triperoxide (TATP), a homemade peroxide-based explosive, is presented. Ion mobility spectrometry (IMS) has proven to be a key analytical technique in the detection of trace explosive material. Unfortunately, IMS alone does not provide chemical identification of the ions detected; therefore, it is unknown what ion species are actually formed and separated by the IMS. In IMS, ions are primarily characterized by their drift time, which is dependent on the ion's mass and molecular cross-section; thus, IMS as a standalone technique does not provide structural signatures, which is in sharp contrast to the chemical and molecular information that is generally obtained from other customary analytical techniques, such as NMR, Raman and IR spectroscopy and mass spectrometry. To help study the ion chemistry that gives rise to the peaks observed in IMS, the hardware of two different commercial IMS instruments has been directly coupled to triple quadrupole (QQQ) mass spectrometers, in order to ascertain each ion's corresponding mass/charge (*m/z*) ratios with different dopants at two temperatures. Isotope labeling was then used to help identify and confirm the molecular identity of the explosive fragment and adduct ions of TATP. The *m/z* values and isotope labeling experiments were used to help propose probable molecular formulas for the ion fragments. In this report, the fragment and adduct ions *m/z* 58 and 240 of TATP have been confirmed to be $[C_3H_6NH \cdot H]^+$ and $[TATP \cdot NH_4]^+$, respectively; while the fragment ions *m/z* 73 and 89 of TATP are identified as having the molecular formulas $[C_4H_9NH_2]^+$ and $[C_4H_9O_2]^+$, respectively. It is anticipated that the work in this area will not only help to facilitate improvements in mobility-based detection (IMS and MS), but also aid in the development and optimization of MS-based detection algorithms for TATP.

Published by Elsevier B.V.

1. Introduction

The organic peroxide, triacetone triperoxide (TATP), Fig. 1a, is a common component of improvised explosive devices (IEDs) used by terrorists [1]. For this reason, there is a great demand for designing or determining methods that can be used to improve the capability and efficiency of detecting TATP, and other compounds in the class of organic peroxides [2,3] The first reported synthesis of TATP was by Wolffenstein in 1895, and its energetic properties were initially attributed to the ether used in the re-crystallization process and not to the TATP itself [4]. In 1959, a more efficient acid-catalyzed synthetic method for activating the ketone (acetone) was described by Milas [5], with variations of this method recently being used by Oxley et al. [6] and Dubnikova et al. [7] TATP exhibits explosive power similar to that of 2,4,6-trinitrotoluene (TNT), and is very sensitive to flame, heat, impact and friction [7–10]. The explosive properties of TATP have been well characterized [7,11] and it has been established that TATP can be detected using analytical methods such as mass spectrometry [3,12]. However, while the signatures used for field detection successfully identify the presence of TATP, a thorough knowledge of the molecular chemistry or product ion formula that is associated

* Corresponding author.
E-mail address: Jason.Stairs@hq.dhs.gov (J. Stairs).

http://dx.doi.org/10.1016/j.talanta.2014.03.044
0039-9140/Published by Elsevier B.V.

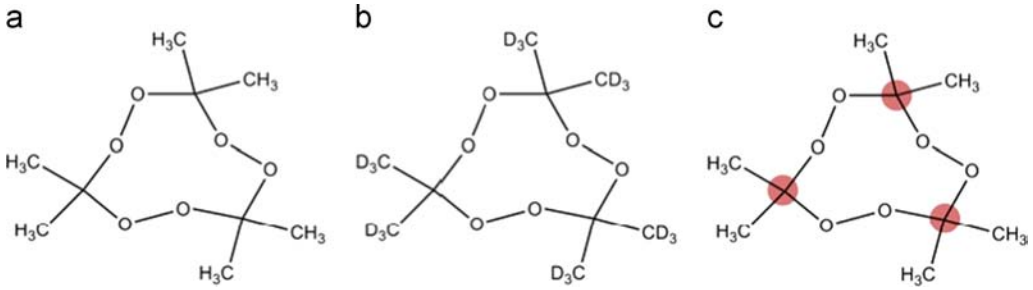

Fig. 1. Chemical structures of (a) TATP, (b) deuterated TATP (d_{18}-TATP), and (c) ^{13}C-TATP, with the labeled ring carbons highlighted (red dots). (For interpretation of the references to color in this figure legend, the reader is referred to the web version of this article.)

with the detection signatures is lacking. Previous studies have been performed in attempts to increase this knowledge; however, results reported to date reveal that there still exists a knowledge gap regarding the chemical or formula identification of the ion chemistry of TATP under atmospheric pressure ionization conditions.

A key and proven analytical method for the field detection of TATP and other contraband is ion mobility spectrometry (IMS), with tens-of-thousands of IMS-based instruments being used by both military and civilian security [13–15]. In many commercial off the shelf (COTS) IMS explosive trace detectors (ETDs), samples of explosive particulates are thermally vaporized, and then ionized by atmospheric pressure chemical ionization (APCI) processes, followed by ion separation based on positive or negative charge, mass, size and geometry. IMS systems identify ions produced in its reaction region (product ions) by their drift time (i.e. mobility value or specific peak positions in the mobility spectrum) as compared to established algorithmic libraries based on empirical data, with the aid of recognition algorithms facilitating TATP detection. When used as a standalone method, IMS does not provide the specificity, resolving power, or molecular signature capability to identify an ion's molecular chemistry or formula.

Most conventional explosives, such as TNT, pentaerythritol tetranitrate (PETN), trinitroglycerin (NG) and 1,3,5-trinitro-1,3,5-triazacyclohexane (RDX), have similar ion chemistry in that they contain active nitro or nitrate functional groups with high electron affinity, giving rise to strong responses in the IMS-negative ion detection mode. The subsequent product ions that are generated for PETN, RDX and NG have been identified to be adducts of the conventional explosive with chloride (Cl^-), nitro (NO_2^-), or nitrate (NO_3^-) ions, while TNT forms M^-, by way of electron loss, when ionized with nitrogen as the only supporting atmosphere or $(M–H)^-$, by way of proton abstraction, in the presence of ions such as O_2^- or Cl^- [16]. The chloride ions are added to the ETDs as a reagent chemical, most commonly as dichloromethane or hexachloroethane, while the formation and presence of the nitro and nitrate adduct groups are attributed to the decomposition of the explosive parent molecules, with the presence of oxygen coming from air. These adduct ions, in turn, act to stabilize other explosive fragments or parent ions, where applicable, aiding in their detection.

TATP displays very different ion chemistries than conventional military explosives. TATP has been shown to generate product ion response peaks in the IMS-negative ion detection mode that have been assigned to mass/charge (m/z) ratios of 143 and 145, of proposed formulas $C_3H_8O_4 \bullet {}^{35}Cl^-$ and $C_3H_8O_4 \bullet {}^{37}Cl^-$, respectively. [17] Unfortunately, this peak response has been shown to be sample dependent, and therefore is unreliable for the detection of pure TATP in the negative ion mode [18].

In contrast, in the IMS-positive ion detection mode, in the presence of isobutyramide (IBA) or ammonia (NH_3) dopants, TATP gives strong product ion peak responses; however, a thorough knowledge of the molecular chemistry or product ion formula that is associated with the IMS peaks of TATP is lacking. A variety of ionization and sample introduction methods and mass spectrometry techniques (i.e., IMS, MS and IMS/MS) have been previously conducted to help address this knowledge gap. These studies have identified product ion m/z ratios for TATP and correlated signatures in TATP detection in attempts to identify the ion chemistry [9,12,18–24]. Specifically, at lower temperatures (i.e. at lower thermal desorption, inlet, and drift temperatures), below ~140 °C, with the ammonia dopant, the m/z 240 peak is prominent and has been identified as having the molecular formula $TATP \bullet NH_4^+$, with a reduced mobility (K_0) of 1.36 $cm^2\,V^{-1}\,s^{-1}$ [9,18–24]. While at higher temperatures, above ~150 °C, either m/z 89 (K_0=2.18 $cm^2\,V^{-1}\,s^{-1}$) [18] or m/z 91 (K_0=2.00 $cm^2\,V^{-1}\,s^{-1}$) [19] tend to dominate; however, only Widmer et al. reported seeing both m/z 89 and 91 peaks in the same experiment [22]. It has been postulated that the m/z 91 peak has the molecular formula $C_3H_6O_3 \bullet H^+$ [19,20,25], while the formula of the m/z 89 peak has yet to be proposed [18,22,23]. Only Marr and Groves [18] reported observing m/z 73 (K_0=2.28 $cm^2\,V^{-1}\,s^{-1}$), however no possible molecular formula was proposed. Shen et al [20], employing the ammonia dopant in their reaction conditions, were the first to attribute the observed m/z 58 (K_0=2.32 $cm^2\,V^{-1}\,s^{-1}$) [18,19] peak to an unknown species and not to the previously assumed molecular formula of acetone $(CH_3)_2C{=}O$, as originally proposed by Marr and Groves [18]. More recently, Ewing et al. [19] has demonstrated that the m/z 58 species is actually due to protonated 2-propanimine, with a molecular formula of $(CH_3)_2C{=}NH \bullet H^+$. The literature reveals that there still exists a paucity of information regarding the chemical or formula identification of the "product ions" of TATP under atmospheric pressure ionization conditions.

To facilitate the chemical identification of the product ions that give rise to IMS peaks in COTS ETDs, the hardware from two COTS IMS-based units has been coupled to triple–quadrupole (QQQ) mass spectrometers (MS). In this recently developed configuration [26], the product ions that are produced in the reaction region of the IMS are passed through an interface region and are detected using either the Faraday plate of the IMS or the mass spectrometer electron multiplier, wherein the product ion intensity is registered as a function of the drift time. By adjusting the operational mode of the mass analyzer, a mobility spectrum and a corresponding mass spectrum (i.e. m/z ratios) can be obtained for the product ions. The full details of the interfacing methodology of these IMS–MS based instruments and the proof of their operational effectiveness in the characterization of TNT, PETN and RDX have been described in previous publications [26,27]. These systems have been employed in this study, along with the chemical additive reagents IBA and ammonia, utilizing the positive ion detection mode, to obtain mobility spectra and corresponding m/z ratios for each product ion of TATP produced. Following mass determinations, isotope labeling experiments were conducted and the isotopic shift results were used to verify the product ions from TATP in

obtained spectra and to help predict possible molecular formulas for these TATP product ions (i.e. for *m/z* 58, 73, 89, 104, 131, 191, and 240). In this document, the integrated Smith Ionscan IMS and Morpho Itemizer ITMS instruments will be referred to as IMS–MS and ITMS–MS, respectively. Briefly stated, the major hardware difference between the two IMS instruments is the ion gate of the IMS instrument versus the ion trap of the ITMS. It is anticipated that the work in this area will not only help to facilitate improvements in mobility-based detection, but also aid in the development and optimization of MS-based detection algorithms [18,19,28] for TATP.

2. Materials and methods

2.1. Disclaimer

TATP is a primary explosive that is highly shock, friction and heat sensitive. Due to the sensitivity of TATP, we recommend that TATP always be synthesized on a small scale and used or disposed of before a new batch is made. It is also recommended that only small samples ($\leq$2.0 g) be handled at a time. Only highly trained and qualified individuals should carry out synthesis of TATP, with safety measures in place (e.g. nitrile gloves, splash goggles with face shield, lab coat and a heavy rubber apron, fume hood, and blast shield). TATP in solution with organic solvents (e.g. methylene chloride, methanol, acetone or hexanes) and water reduces the compound's sensitivity. Crystals and solutions of TATP should always be stored in non-threaded plastic containers, inside a chemical refrigerator, as threads possess a risk of friction ignition when opening. Refrigeration can suppress friction and heat related ignition events, TATP sublimation as well as the conversion of TATP to Diacetone Diperoxide (DADP).

2.2. General methods and materials

All reactions were carried out in a fume hood, under temperature conditions that ranged from −20° to 25 °C, utilizing a 50 mL plastic beaker, a Teflon-coated magnetic stir bar, appropriate personal protection equipment (PPE) and a blast shield. The 50 mL plastic beaker was always secured within a secondary plastic container that served as a cooling and overflow container. The 50 mL plastic beaker's reaction (solution) temperature was continuously monitored by inserting a glass thermometer directly into the solution. Deuterium labeled acetone (Acetone-d_6, 99.9% purity) and ^{13}C-labeled acetone (Acetone-2-^{13}C, 99% purity) were purchased from Cambridge Isotope Laboratory Inc., Andover, MA. Methylene chloride (CHROMASOLV®, for HPLC, ≥99.9%,), methanol (CHROMASOLV®, for HPLC, ≥99.9%), hexanes (CHROMASOLV®, for HPLC, ≥98.5%), acetonitrile (CHROMASOLV® Plus, for HPLC, ≥99.9%) and acetone (CHROMASOLV® Plus, for HPLC, ≥99.9%) were all purchased from Sigma-Aldrich and used as purchased. Hydrogen peroxide (50 wt% in H_2O, ACS reagent) and Sulfuric acid (18 M) were purchased from Sigma-Aldrich. Unlabeled (NH_3) and labeled (ND_3 and $^{15}NH_3$) ammonia permeation tubes were purchased from Real Sensors, Hayward, CA. The IBA permeation tube was provided by Smiths Detection, Inc., Toronto, ON, Canada. The theoretical and experimental Raman spectra for TATP and d_{18}-TATP can be found in Fig. S1 and in our previous publication [29].

2.3. Synthesis of TATP ($C_9H_{18}O_6$)

Preparation of TATP followed the methods of Milas [5], Oxley et al [6] and Dubnikova et al. [7], with modifications as follows: Acetone (4.0 mL, 3.16 g, 54.5 mmol) was added to a 50 mL plastic beaker that had been cooled to −20 °C. The plastic beaker was cooled by immersing it in a secondary container that contained an acetone–dry ice bath. A glass thermometer was directly inserted inside the acetone reagent solution and its temperature was monitored until it reached −20 °C. With continuous stirring, hydrogen peroxide (1.6 mL, 1.78 g, 52.2 mmol) was slowly added to the acetone reagent. Once the solution mixture reached −20 °C again, 0.4 mL of concentrated sulfuric acid (18 M) was added very slowly (drop-wise) to the reaction mixture, using a long-tipped Pasteur pipette, making sure to keep the temperature below −10 °C. If the temperature rose above −10 °C, the addition of acid was stopped until the reaction mixture cooled to −20 °C again, before more acid was added. This procedure was continued until all of the acid was added. Addition of acid took approximately 10 min; to hurry the process would invite a violent rapid heating event accompanied by vigorous solution bubbling and overflow. After all the acid had been added, the reaction vessel temperature was slowly brought up to 0 °C over 20 min, and then allowed to stir for an additional 10 min at 0 °C and 25 °C (room temperature), respectively. During warming of the reaction mixture, product progressively formed and precipitated out of solution as a white solid.

After stirring for 10 min at room temperature, methylene chloride (15 mL) was added to the reaction vessel to dissolve the product. The full contents of the reaction mixture were transferred to a separatory funnel and washed with 10 mL portions of refrigerated DI water until the pH of the organic layer was between 6 and 7. The organic layer was then emptied onto a petri dish that was placed behind a blast shield inside the fume hood and the solvent was allowed to evaporate until the sample was virtually dry. Using a plastic spatula, the white solid accumulation was transferred onto a frit and washed with 2.0 mL of cold DI water, and suction dried. TATP (2.33 g) was obtained as a white microcrystalline powder after drying under reduced pressure [57.8 % yield based on acetone]. The product was further crystallized as large transparent crystals by dissolving the white microcrystalline powder into a minimum amount of hexanes or pentanes solvent and allowing the solution to sit in the freezer (between 0 °C and 5 °C) overnight. TATP crystals were stored in the freezer until used.

2.4. Synthesis of deuterated TATP ($C_9D_{18}O_6$)

d_{18}-TATP was synthesized following the same procedure described above for unlabeled TATP, except deuterated acetone (Acetone-d_6, 99.9% purity) was substituted.

2.5. Synthesis of ^{13}C-labeled TATP ($^{13}C_3C_6H_{18}O_6$):

^{13}C-TATP was synthesized following the same procedure described above for unlabeled TATP, except ^{13}C-labeled acetone (Acetone-2-^{13}C, 99% purity) was substituted.

2.6. Preparation of TATP Test Samples

TATP crystal samples (1–10 ug) were used in IMS, IMS–MS and ITMS–MS analysis. Crystalline samples were used to minimize or eliminate any solvent influence [30]. Crystals were placed directly onto a Teflon sample trap and inserted into the thermal desorber. In order to prevent any significant TATP loss due to sublimation, time allowed between deposition of TATP crystals onto a Teflon sample trap and thermal desorption was on the order of a few seconds. Unless specified below, the instrument parameters used to collect the TATP spectra are identical to those found in our previous publications [26,27]. In addition to wearing the required PPE (e.g. nitrile gloves, safety goggles, lab coat, etc.), an electrostatic discharge (ESD) bracelet was worn and a ESD mat was used

to ensure a proper instrument grounding source and to prevent static build up that could cause ignition of the TATP crystals.

3. Results and discussion

3.1. IBA and NH_3 signatures in IMS–MS and ITMS–MS

The two standalone COTS IMS and ITMS ETDs use IBA and ammonia additives to aid in product ion formation, stabilization and detection; thus the ion chemistry associated with both reagents was evaluated. IBA and ammonia are used in positive ion detection mode because of their strong proton affinities of 878.6 kJ/mol and 853.6 kJ/mol, respectively [23], and due to observations that these reagents produce good sensitivity and selectivity in this detection mode. Employing our instrumental conditions, it was determined that IBA produces two characteristic mass spectrum peaks of *m/z* 88 and 175. The *m/z* 88 peak is attributed to a protonated IBA monomer, $IBA{\bullet}H^+$, while the *m/z* 175 peak is attributed to a protonated IBA dimer, $(IBA)_2{\bullet}H^+$. Due to its high proton affinity and the readily available protons from the carrier gas, ammonia exists in the IMS reaction chamber as a reactant ion in its protonated ammonium ion form, ($NH_3{\bullet}H^+$). Ammonium ion response peaks at *m/z* 18 and *m/z* 35 were not observed due to instrument limitations (i.e. low mass cutoff). A survey of the literature revealed no publications on the IMS or MS response for TATP with the IBA additive; hence, the response of TATP in the presence of IBA was considered in this study and compared to the response produced when NH_3 was used.

3.2. TATP mobility spectra comparison and spectroscopic compound characterization

Pure intact (molecular) TATP is a well-known compound and has been previously characterized by Oxley et al. (^{1}H and ^{13}C-NMR) [6] and more extensively by Buttigieg et al. (^{1}H and ^{13}C-NMR, RTIR and Raman Spectroscopy, as well as IMS and IMS–MS in the absence of additive reagents) [31]. To support previous analytical results and to aid in further TATP characterization regarding its product ion chemistry after IMS atmospheric pressure chemical ionization, IMS–MS and ITMS–MS mobility spectra were obtained. Representative IMS–MS and ITMS–MS mobility spectra for TATP, with our corresponding *m/z* ratio assignments, Fig. 2, were collected under each instrument's optimized high temperature conditions, Table 1, using IBA and ammonia additive reagents in positive ion detection mode.

The temperatures provided in Table 1 were instrument set temperatures and not the actual air temperature readings, thus one may anticipate some minor variations between air temperature and the instrument setting temperature. Due to instrument configurations, it was not possible to measure gas temperature while taking measurements. It may also be noted that the high temperature settings for the IMS–MS and ITMS–MS instruments are different, as these are the manufacturer specified temperatures for the COTS instruments.

The mobility spectra of TATP from the standalone COTS IMS ETDs were also obtained and compared to those in Fig. 2; the peaks obtained from the standalone ETDs and the IMS–MS and ITMS–MS instruments were in near identical agreement. This result not only provides evidence that the IMS portion of the IMS–MS and ITMS–MS instruments exhibit the same ion chemistry of interest for TATP, but also confirms that the IMS–MS and ITMS–MS instruments were functioning accurately for TATP product ion detection, as previously established for TNT, PETN and RDX, using these integrated configurations [26,27]. In addition, the reduced mobility values calculated for TATP product ions produced by the integrated systems were in good agreement with literature, Table 2, providing additional evidence that the same ion chemistry reactions for TATP are occurring in our instrument configurations. The mobility spectra in Fig. 2 reveal that the prominent mobility peak observed in IMS–MS is *m/z* 89 (K_0=2.17 cm^2/V s), with *m/z* 58 (K_0=2.35 cm^2/V s) being the prominent mobility peak in ITMS–MS, under our experimental instrument conditions. The reduced mobility, K_0, values were calculated by normalizing the drift time of the analyte to the drift time of cocaine (K_0=1.16 cm^2 V^{-1} s^{-1}) [32],cocaine was selected due to its common use in IMS.

The agreements of the mobility spectra and calculated reduced mobility (K_0) also confirm the synthetic procedure employed to synthesize TATP, which is a slight modification on the synthetic procedures used by Milas, Oxley and Dubnikova. In addition, Raman spectra results of pure and deuterated TATP (d_{18}-TATP) samples, synthesized using the experimental procedure reported herein, were compared to theoretical Raman spectra of both the parent and deuterated isotopologue. The theoretical Raman spectra, see Fig. S1, were predicted using density functional theory calculations, employing the EDF2/6-311++G** and B3LYP/6-311++G** level of theory and methods (basis sets). As illustrated in Fig. S1, the experimental Raman spectra for TATP and d_{18}-TATP are in near identical agreement with the theoretical spectra, and

Table 1
Temperature settings for the standalone and integrated instruments.

Hardware	COT IMS and IMS–MS	COT ITMS and ITMS–MS
High temperature settings		
Desorbers	205 °C	220 °C
Inlet tubes	285 °C	n/a
Drift tubes	220 °C	162 °C
Low temperature settings		
Desorbers	100 °C	100 °C
Inlet tubes	100 °C	n/a
Drift tubes	100 °C	100 °C

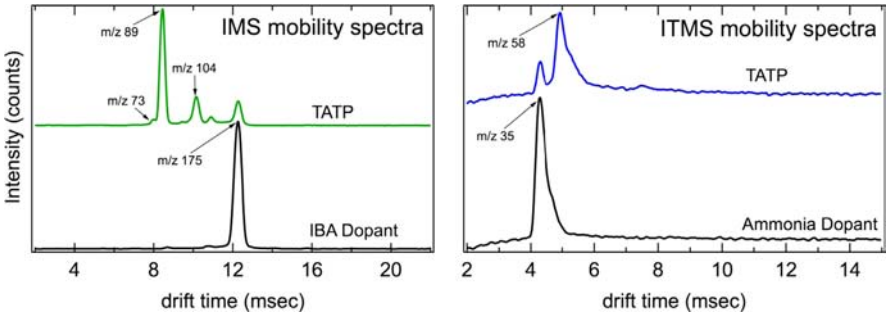

Fig. 2. The high temperature IMS–MS mobility spectrum of TATP with the IBA dopant (left) and the high temperature ITMS–MS mobility spectrum of TATP with the NH_3 dopant (right) are compared to the pure dopant background spectra (bottom traces).

the corresponding deuterium isotopic shifts for the vibration modes are listed in Table S1. The agreement in the experimental and theoretical Raman results provides additional evidence that TATP was synthesized in pure form. These results were previously reported in detail [29].

3.3. High and low temperature IMS–MS and ITMS–MS mass spectra of TATP and reactant ion affects

IMS–MS mass spectra were collected for TATP at both high and low temperatures (Table 1), in the presence of IBA and unlabeled (NH_3) and labeled (ND_3) ammonia dopant, Fig. 3. The analogous high and low temperature ITMS–MS mass spectra, utilizing unlabeled ammonia, are shown in Fig. 4. Expanded views of the high and low mass region of the IMS–MS spectra of Fig. 3 are illustrated in Fig. 5, wherein the spectrum results using ^{15}N-labeled ammonia ($^{15}NH_3$) as a dopant have been included for comparison. In the IMS–MS configuration, employing our high temperature

Table 2
Calculated reduced mobility values, K_0, for each of the IMS peaks identified.

m/z	K_0 from IMS–MS with IBA (cm^2/V s)	K_0 from ITMS–MS with NH_3 (cm^2/V s)	Literature K_0 (cm^2/V s)
58	Not measured	2.35	2.32 [18,19]
73	2.30	2.28	2.28 [18]
89	2.17	2.21	2.18 [18]
91	n/a	2.08	2.08 [19]
104	1.78	n/a	n/a
144	1.69	n/a	n/a
191	1.58	n/a	n/a

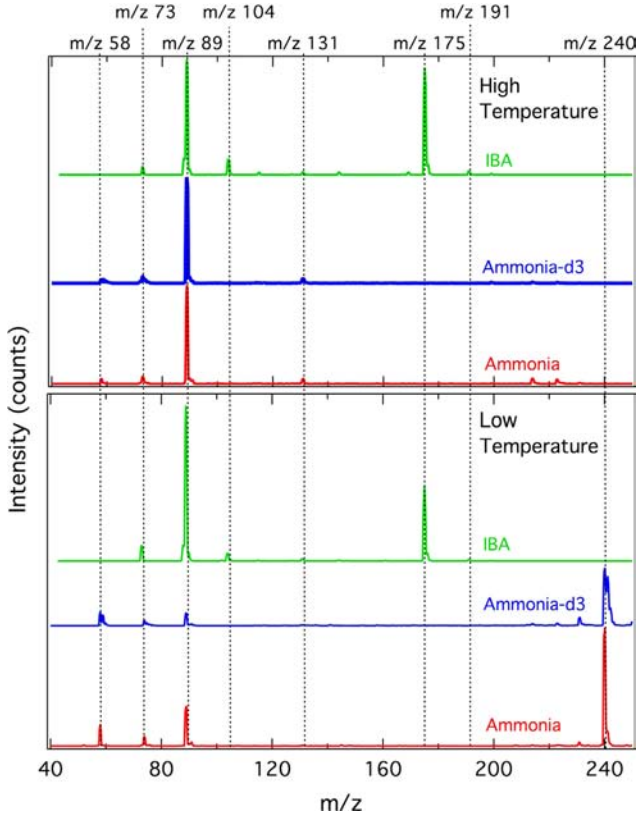

Fig. 3. The IMS–MS mass spectra of TATP in the presence of the IBA (green), NH_3 (red) and ND_3 (blue) dopants, under high temperature (upper panel) and low temperature (lower panel) conditions. (For interpretation of the references to color in this figure legend, the reader is referred to the web version of this article.)

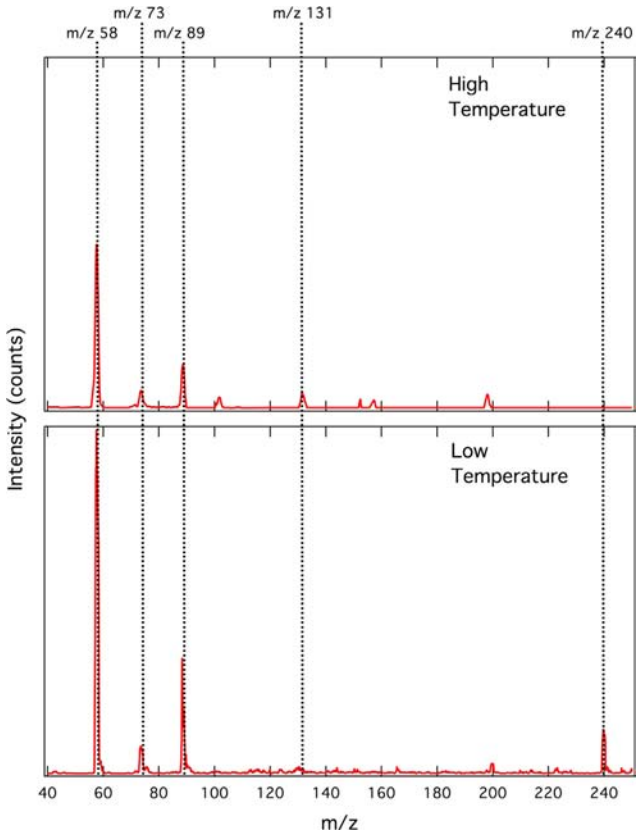

Fig. 4. The ITMS–MS mass spectra of TATP in the presence of the NH_3 additive, under high temperature (upper panel) and low temperature (lower panel) conditions.

conditions, TATP product ions *m/z* 73, 89 and 131 are produced in the presence of IBA, NH_3 and ND_3, with *m/z* 58 being produced in the presence of NH_3 and ND_3 and *m/z* 89 being the prominent peak in all three spectra, Fig. 3 (top spectra). Mass ratios of *m/z* 104, 175 and 191 were only observed in the presence of IBA at high temperature. We attribute the *m/z* 175 peak to the protonated IBA dimer, $(IBA)_2 \bullet H^+$. At this point, the identities of the *m/z* 104 and 191 peaks are unclear. However, in contrast to what is observed for the other ion peaks, it has been determined that the *m/z* 104 and 191 peaks do not exhibit isotopic shifts in the corresponding d_{18}-TATP or ^{13}C-TATP IMS–MS spectra, Figs. 6 and 7, respectively, suggesting that these species do not contain any hydrogen or carbon atoms from TATP. At high temperature, no *m/z* 240 peak was observed in the presence of IBA, NH_3 or ND_3.

Under low temperature conditions, TATP product ions 73, 89 and 131 were also produced in the presence of IBA, NH_3 and ND_3, with *m/z* 58 being produced in the presence of NH_3 and ND_3 Fig. 3 (bottom spectra). In the presence of NH_3 and ND_3, the *m/z* 89 peak significantly decreased in intensity, and the *m/z* 240 peak became the prominent product ion peak in the spectra. With IBA at lower temperature, *m/z* 89 remained the prominent product ion peak and the peak intensity for *m/z* 191 increased, with no peak being observed for *m/z* 240 in this spectrum. Despite running several IMS–MS low temperature experiments, as low as 80 °C, no peak for a proposed (TATP-IBA$\bullet H^+$) adduct at *m/z* 310 was observed. The ITMS–MS configuration gave similar results as the IMS–MS instrument, under low and high temperature conditions, in the presence of unlabeled ammonia, Fig. 4, indicating that similar reactions are occurring in both instruments. Based on this result, IBA, ND_3 and $^{15}NH_3$ with TATP were not evaluated with the ITMS–MS configuration. In the ITMS–MS configuration, it was observed that the *m/z* 58 product ion peak was the major peak produced instead of the *m/z* 89 product ion peak, in the presence of NH_3 at

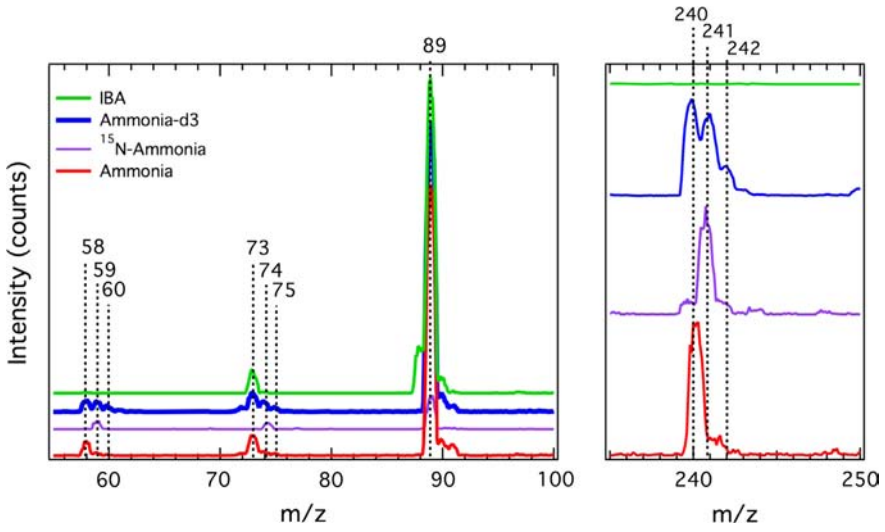

Fig. 5. Expanded views of the high and low mass region of the IMS–MS spectra of Fig. 3. Displayed are the IMS–MS mass spectra of TATP in the presence of the IBA (green), NH_3 (red), ND_3 (blue), and ^{15}N-labeled ($^{15}NH_3$, purple) additives, under high temperature conditions (left) and low temperature conditions (right). Note: the multiple peaks that appear for ND_3 are indicative of hydrogen–deuterium proton exchange and the single peak isotopic $^{15}NH_3$ shifts are indicative of nitrogen atom association or incorporation. (For interpretation of the references to color in this figure legend, the reader is referred to the web version of this article.)

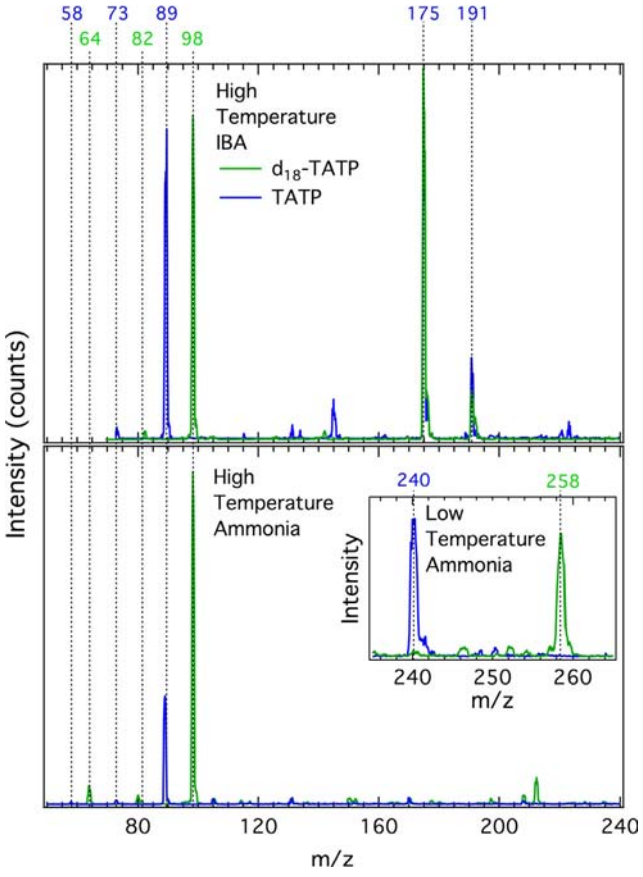

Fig. 6. Mass spectra of TATP (blue) and d_{18}-TATP (green) with IBA (upper panel) and NH_3 (lower panel) using IMS–MS, under high temperature conditions. Inset shows the mass spectra of TATP (blue) and d_{18}-TATP (green) with NH_3 under low temperature conditions in the IMS–MS. (For interpretation of the references to color in this figure legend, the reader is referred to the web version of this article.)

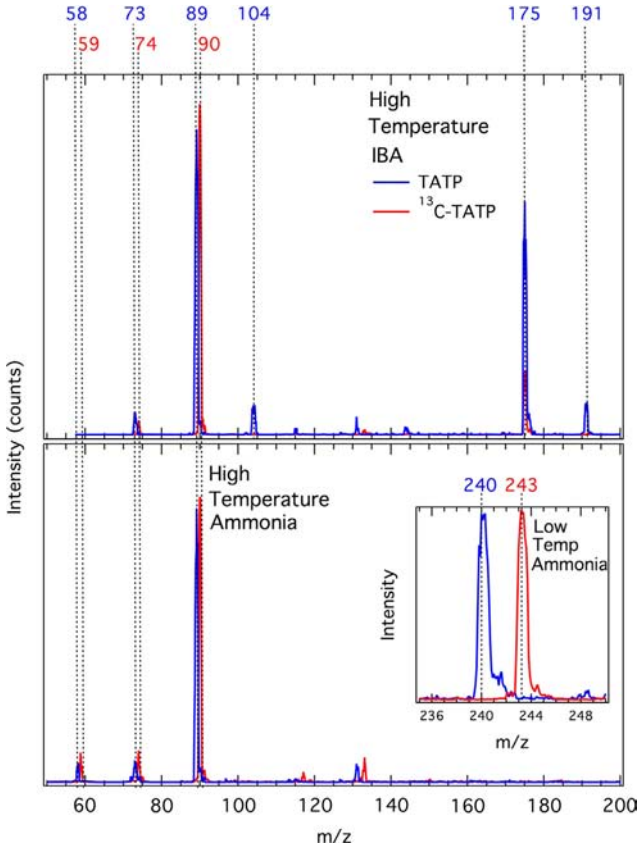

Fig. 7. Mass spectra of TATP (blue) and ^{13}C-TATP (red) with IBA (upper panel) and NH_3 (lower panel) using IMS–MS, under high temperature conditions. Inset shows the mass spectra of TATP (blue) and ^{13}C-TATP (red) with NH_3 under the low temperature conditions in the IMS–MS. (For interpretation of the references to color in this figure legend, the reader is referred to the web version of this article.)

low and high temperatures, Fig. 4. This is believed to be due to the longer time the molecules and ions spend in the ionization region of the ITMS–MS relative to that of the IMS–MS configuration (i.e. the ions spend more time in the ionization region of the ITMS–MS due to the utilization of the ion trap). However, we cannot discount any role that the slightly higher desorption and lower drift temperatures of the ITMS–MS system may play on product ion formation, Table 1.

When the ND_3 dopant was used, multiple peaks were observed for the *m/z* 58, 73 and 240 product ion peaks, Fig. 5. In the presence of the $^{15}NH_3$ ammonia additive, a single peak shift of one

mass unit for each product ion, *m/z* 58, 73 and 240, was observed, purple spectrum in Fig. 5. The ^{15}N-labeled results indicate that each product ion is associated with or contains a nitrogen atom. In the case of the ND_3 additive, we attribute multiple peak formation for *m/z* 58, 73 and 240 to hydrogen–deuterium proton exchange taking place. The deuterated ammonium ion ($ND_3 \bullet H^+$) is exchanging deuterium atoms with the proton rich atmosphere (e.g. $H_3O^+ \bullet xH_2O$ clusters) of the reaction region before or after $ND_3 \bullet H^+$ reacts with TATP or TATP product ions, yielding $-ND_3$, $-NHD_2$, $-NH_2D$, or $-NH_3$ substitution or adduct type products. The observed isotopic shifts and multiple peak formations, after using the ND_3 and $^{15}NH_3$ additives, verify that TATP and/or its fragment product ions are reacting with the ammonia dopant during the atmospheric pressure chemical ionization processes. Although we cannot rule out some contribution from hydrogen–deuterium proton exchange at this point, we attribute the minor intensity shoulder peaks associated with *m/z* 89 to a ^{13}C-natural abundance contribution (i.e. *m/z* 90) and to the direct formation of an additional TATP product ion (i.e. *m/z* 91), both of which have previously been observed [19–22,25,33].

3.4. TATP isotope labeling experiments and MS–MS analysis

3.4.1. High and low temperature IMS–MS mass spectra of d_{18}-TATP and ^{13}C-TATP: product ion molecular formula determination for observed peaks.

To further verify the product ion peaks that are directly associated with the hydrogen and carbon constituents of TATP in obtained spectra, and to assist in the identification of their corresponding molecular formulas, isotopic labeling experiments were conducted, and the resultant isotopic shifts for *m/z* ratios 58, 73, 89 and 240 were acquired. The d_{18}-TATP and ^{13}C-TATP IMS–MS spectra were attained at low and high temperatures, in the presence of the IBA and NH_3 dopants, Figs. 6 and 7, respectively. In the absence of an additive reagent, it has been demonstrated that the parent TATP molecule exhibits a *m/z* ratio of 223, when it is ionized in a proton rich atmosphere, yielding a corresponding molecular formula of $TATP \bullet H^+$ [6,23,31]. Under low temperature conditions, in a proton rich atmosphere, a *m/z* ratio of 240 is observed when TATP is ionized in the presence of NH_3, inset illustration in Figs. 6 and 7. During the synthesis of ^{13}C-TATP, only the ring carbon atoms of TATP are labeled, as a result of using 2-^{13}C-labeled acetone. A structural representation of ^{13}C-TATP is shown in Fig. 1c, where the ^{13}C-carbons are highlighted in red. The following sections will provide a more detailed account of the isotopic shifts observed for each *m/z* ratio. Although the *m/z* 131 product ion was observed at low and high temperatures, Figs. 3 and 4, it is important to note that its appearance and its observed isotopic shifts were inconsistent under our experimental conditions. Thus, at this time, the chemical identity of the *m/z* 131 product ion is not determined.

3.4.2. m/z 240 adduct ion peak

In the absence of an additive reagent, the expected isotopic shift for full deuterium substitution of the parent TATP molecule is from 222 amu to 240 amu (d_{18}-TATP), a mass difference of 18 amu. When TATP is ionized in the presence of NH_3 at low temperature, a *m/z* ratio of 240 is observed, which is also a mass difference of 18 amu, and in this case represents the mass of the protonated ammonium ion, ($NH_3 \bullet H^+$) adduct, Figs. 6 and 7. Under low temperature conditions with NH_3 and d_{18}-TATP, a *m/z* ratio of 258 is obtained, Fig. 6, bottom inset. The observed *m/z* ratio of 258 is a total mass shift of 36 amu from that of 222 for the parent TATP molecule, confirming full deuterium substitution of the eighteen hydrogen atoms of TATP and the contribution of the protonated ammonium ion, ($NH_3 \bullet H^+$), to the overall mass. With the ND_3 dopant and TATP, the single *m/z* 240 peak split into multiple peaks, Fig. 5, verifying that the ammonia reagent does in fact coordinate to TATP, yielding ($TATP \bullet ND_{3-x}H_xH^+$) type products. When isotopically labeled $^{15}NH_3$ was used as the additive, a shift from *m/z* 240 to *m/z* 241 was observed, Fig. 5; this result reveals a single nitrogen association and provides additional proof of ammonia coordination. In the low temperature ^{13}C-TATP spectrum, Fig. 7 (inset), the *m/z* 240 peak shifted to *m/z* 243, confirming ^{13}C-labeling of the three ring carbon atoms of the parent TATP molecule and retention of its molecular structure. In the deuterated spectra of Figs. 6 and 7, the *m/z* 240 product ion was not observed under high temperature conditions in the presence of IBA or NH_3.

Utilizing the tandem mass spectrometry (MS–MS) mode of the IMS–MS and ITMS–MS instruments, the unlabeled *m/z* 240 product ion peak fragmented, producing daughter ion peaks of *m/z* 223, 148, 132, 91, 74 and 43 in both the IMS–MS and ITMS–MS configurations; the daughter ions produced are consistent with previous findings for daughter ions of *m/z* 240 [9,22,23]. We attribute the *m/z* 223 daughter ion to having a molecular formula of $TATP \bullet H^+$, with this assignment being supported by previous published results [6,23,31]. The formation of $TATP \bullet H^+$ during MS–MS fragmentation confirms the presence of TATP in the *m/z* 240 adduct. It is noteworthy that Shen et al. identified the *m/z* 74 and 91 daughter ions as having molecular formulas of $C_2H_6O_2^+$ and $C_3H_6O_3 \bullet H^+$, respectively [20], with the *m/z* 91 peak recently being observed under the experimental conditions employed by Ewing et al. [19] It has been hypothesized that the MS–MS daughter ion of *m/z* 43 is due to $(CH_3)CO^+$ [20,21,24,25,34]. Based on the results presented here, the molecular formulas of the *m/z* 240, 243 and 258 product ions are attributed to ammonium adducts $TATP \bullet NH_4^+$, $^{13}C\text{-}TATP \bullet NH_4^+$ and $d_{18}\text{-}TATP \bullet NH_4^+$, respectively. These results also confirm previous literature reports that $TATP \bullet NH_4^+$ is a major product ion formed in the presence of the ammonia dopant, employing our low temperature experimental conditions.

3.4.3. m/z 58 product ion peak

As demonstrated above, a product ion peak with an *m/z* ratio of 58 is observed in the IMS–MS and ITMS–MS spectra, Figs. 3 and 4 respectively, when TATP is ionized in the presence of NH_3, under low and high temperature conditions. Despite the temperature conditions, the *m/z* 58 product ion is not observed in the presence of IBA. In the IMS–MS high temperature spectra of d_{18}-TATP, also in the presence of NH_3, a deuterium shift from *m/z* 58 to *m/z* 64 is observed, Fig. 6. The corresponding deuterium mass shift is 6 amu, indicative of the *m/z* 64 product retaining two deuterated methyl groups [$(-CD_3)_2$ i.e. (C_2D_6)] from d_{18}-TATP, revealing that the original *m/z* 58 product ion contains a $[C_2H_6]$ molecular component. In the IMS–MS ^{13}C-TATP spectrum, under the same conditions, the *m/z* 58 peak shifted to *m/z* 59, Fig. 7, confirming that one of the ^{13}C-carbon atoms from the three ring carbons of TATP was present, producing an extended one carbon molecular component of $[C_2H_6C]$. To investigate the presence of nitrogen in the *m/z* 58 product ion, an IMS–MS spectrum of TATP was collected in the presence of $^{15}NH_3$. In this case, a shift of the product ion from *m/z* 58 to *m/z* 59 was observed, Fig. 5, confirming that the *m/z* 58 ion contains a nitrogen atom, yielding an extended molecular component of $[C_2H_6CN]$. When TATP was ionized in the presence of ND_3, it was observed that the single *m/z* 58 product ion peak split into multiple peaks, Fig. 5, verifying that this product ion contains multiple hydrogen atoms that are capable of undergoing hydrogen–deuterium exchange. The multiple peaks can be attributed to the presence of two interchangeable hydrogen atoms as follows: *m/z* 58 would contain two hydrogen atoms, *m/z* 59 would contain

one hydrogen and one deuterium, and *m/z* 60 would contain two deuterium atoms; thus exhibiting a molecular component of $[C_2H_6CNH_2]$.

MS–MS analysis of the *m/z* 58 and deuterated *m/z* 64 product ions produced single daughter ion peaks at *m/z* 43 and *m/z* 46, respectively. The *m/z* 46 daughter ion peak exhibits the expected isotopic peak shift of 3 amu, representative of a (CH_3) group being present in the original *m/z* 43 daughter ion (i.e. in the corresponding *m/z* 58 product ion). MS–MS analysis of the ^{13}C-labeled (*m/z* 59) and ^{15}N-labeled (*m/z* 59) product ions both produced a daughter ion peak at *m/z* 44, yielding the expected 1 amu isotopic shift from the *m/z* 43 peak in both cases, confirming that one of the ring carbons from TATP and a nitrogen atom is present in the *m/z* 58 product ion. Based on the isotopic labeling experiments and MS–MS data presented, and considering the efficiency of the atmospheric pressure chemical ionization processes, we concluded that the *m/z* 58 product ion has a molecular formula of $C_3H_6NH{\bullet}H^+$, which is the formula for protonated 2-propanimine, $(CH_3)_2C{=}NH{\bullet}H^+$ as proposed by Ewing et al., where he also postulated the mechanism of formation. [19] Our *m/z* assignment of 58 and isotopic labeling experiments provide additional support for the results published by Ewing et al., with the isotope ^{15}N-labeling experiment in particular validating Ewing's assumption that the *m/z* 58 product ion contains only one nitrogen.

As stated above, the *m/z* 43 ion has been hypothesized previously as having a molecular formula of $(CH_3)CO^+$ [20,21,24,25,34]. However, based on our data and the results published by Ewing et al., we hypothesize that the MS–MS *m/z* 43 daughter ion in this case is formed by alpha cleavage of a methyl group from protonated 2-propanimine, $(CH_3)_2C{=}NH{\bullet}H^+$, leading to the formation of a $[(CH_3)CNH_2{\bullet}^+]$ radical cation fragment, under our experimental conditions. Thus, we infer that the *m/z* 43 daughter ion obtained from *m/z* 58 is different than the *m/z* 43 daughter ion that came from *m/z* 240 (section 3.4.2) and different from the previously proposed formula of $(CH_3)CO^+$.

In Ewing's report [19], it was shown that excess ammonia causes the major *m/z* 240 product ion peak to significantly decrease, resulting in a large increase in the production of the *m/z* 58 peak. Ewing et al. concluded that this was the direct result of a NH_3 driven reaction, initiated by increasing the concentration of ammonia from 4.7 ppm_v to 8.1 ppm_v at 80 °C. To further test this hypothesis, the gas phase chemical ionization of acetone, $(CH_3)_2C{=}O$, in the presence of ammonia was investigated by Ewing et al. [19]. In this experiment, the *m/z* 58 product ion was produced in high intensity, providing additional evidence for the formation of $(CH_3)_2C{=}NH{\bullet}H^+$. The structural computational work of Sigman et al. [21]. revealed that proton interaction with a TATP oxygen in $TATP{\bullet}H^+$ results in extensive lengthening of the C–O bond to 2.605 Å, indicative of weakening of the C–O bond upon proton coordination [21]. It is expected that weakening of a C–O bond in $TATP{\bullet}NH_4^+$ would also occur upon coordination of $(NH_3{\bullet}H^+)$ to a TATP oxygen. The binding energy in $TATP{\bullet}NH_4^+$ was calculated by Sigman et al. [21]. to be 25 kcal/mol, compared to an O–O bond energy of ~36 kcal/mol in TATP [6,7], indicating that ammonia coordination is stable. Based on their results and the computational data, Ewing et al. proposed a likely mechanism that involved the interaction of $TATP{\bullet}NH_4^+$ with excess NH_3, leading to the production of protonated 2-propanimine [19], Fig. 8. Ewing et al. [19]. also observed the formation of *m/z* 91 as a second major product ion peak under their experimental conditions. We also propose that *m/z* 58 $(C_3H_6NH{\bullet}H^+)$ is primarily formed by additional NH_3 reacting directly with $TATP{\bullet}NH_4^+$; however, we have not ruled out the possibility of a small contribution to its formation resulting from an acid catalyzed background reaction, wherein NH_3 reacts with activated acetone, $(CH_3)_2C{=}O$, in our proton rich environment.

3.4.4. *m/z* 73 product ion peak

The IMS–MS spectrum of TATP exhibits a low intensity peak at *m/z* 73, under high and low temperature conditions, when TATP is ionized in the presence of IBA and NH_3, Figs. 3 and 4. In the IMS–MS high temperature spectra of d_{18}-TATP, in the presence of IBA and NH_3, a deuterium shift from *m/z* 73 to *m/z* 82 is observed, Fig. 6. The corresponding deuterium mass shift is 9 amu, indicative of the *m/z* 82 product retaining three deuterated methyl groups $[(-CD_3)_3$ i.e. $(C_3D_9)]$ from d_{18}-TATP, revealing that the original *m/z* 73 product ion contains a $[C_3H_9]$ molecular component. In the IMS–MS ^{13}C-TATP spectrum, under the same conditions, the *m/z* 73 peak shifted to *m/z* 74, Fig. 7, confirming that one of the ^{13}C-carbon atoms from the three ring carbons of TATP was present, producing an extended one carbon molecular component of $[C_3H_9C]$. To investigate the presence of nitrogen in the *m/z* 73 product ion, an IMS–MS spectrum of TATP was collected in the presence of $^{15}NH_3$. In this case, a shift of the product ion from *m/z* 73 to *m/z* 74 was observed, Fig. 5, confirming that the *m/z* 73 ion contains a nitrogen atom, yielding an extended molecular component of $[C_3H_9CN]$. When TATP was ionized in the presence of ND_3, it was observed that the single *m/z* 73 product ion peak split into multiple peaks, Fig. 5, verifying that this product ion contains multiple hydrogen atoms that are capable of undergoing hydrogen–deuterium exchange. The multiple peaks can be further attributed to the presence of two interchangeable hydrogen atoms as follows: *m/z* 73 would contain two hydrogen atoms, *m/z* 74 would contain one hydrogen and one deuterium, and *m/z* 75 would contain two deuterium atoms; thus exhibiting a molecular component of $[C_3H_9CNH_2]$.

MS–MS analysis of the *m/z* 73 and deuterated *m/z* 82 product ions produced single daughter ion peaks at *m/z* 43 and *m/z* 46, respectively. The *m/z* 46 daughter ion peak exhibits the expected isotopic peak shift of 3 amu, representative of a methyl group, (CH_3), being present in the original *m/z* 43 daughter ion (i.e. in the corresponding *m/z* 73 product ion). MS–MS analysis of the ^{13}C-labeled (*m/z* 73) and ^{15}N-labeled (*m/z* 73) product ions both

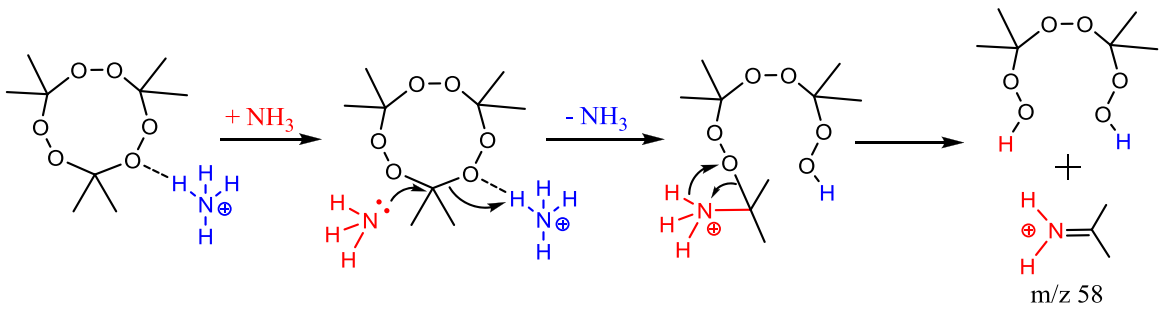

Fig. 8. Proposed reaction scheme adapted from Ewing et al. [19]. for the formation of the *m/z* 58 product ion.

produced a daughter ion peak at *m/z* 44, yielding the expected 1 amu isotopic shift from the *m/z* 43 peak in both cases, confirming that one of the ring carbons from TATP and a nitrogen atom is present in the *m/z* 73 product ion. Based on the isotopic labeling experiments and MS–MS data presented, and considering the atmospheric pressure chemical ionization processes, we postulate that the *m/z* 73 product ion has a molecular formula of $C_3H_9CNH_2{\bullet}^+$, with a proposed structural formula of the tert-butylamine radical cation, $(CH_3)_3C-NH_2{\bullet}^+$. Due to the ^{15}N-labeled MS–MS result, we also propose that the *m/z* 43 daughter ion in this case has the same molecular formula [$(CH_3)CNH_2{\bullet}^+$] as that of the MS–MS breakdown product of *m/z* 58, resulting from the loss of two methyl radicals, ($CH_3{\bullet}$), from the tert-butylamine radical cation $(CH_3)_3C-NH_2{\bullet}^+$ species.

Radical cations are well studied and their chemistry was reviewed by Schmittel and Burghart over a decade ago [35]. McCormick et al. demonstrated that thermal desorption of tert-butylamine yielded product ion peaks at *m/z* 57, 58, 73 and 74, after analyzing desorption products by field-ionization mass spectroscopy [36]. The peak at *m/z* 57 was attributed to a tert-butyl ion species. The *m/z* 73 peak was assigned to the tert-butylamine radical cation $(CH_3)_3C-NH_2{\bullet}^+$. McCormick et al. proposed that the *m/z* 58 peak was protonated 2-propanimine, $(CH_3)_2C{=}NH{\bullet}H^+$, formed by alpha cleavage of a methyl radical ($CH_3{\bullet}$) from the tert-butylamine radical cation $(CH_3)_3C-NH_2{\bullet}^+$. The *m/z* 74 peak was assigned to protonated tert-butylamine $(CH_3)_3C-NH_2^+$. In a parallel study, Hammerum and Derrick reported that the conversion of protonated 2-propanimine, $(CH_3)_2C{=}NH{\bullet}H^+$, from the tert-butylamine radical cation, $(CH_3)_3C-NH_2{\bullet}^+$, by alpha cleavage of a methyl radical ($CH_3{\bullet}$), proceeds with a translational energy release of 11 kJ mol^{-1} [37]. Thus, they concluded that the reverse reaction of methyl radical ($CH_3{\bullet}$) addition to $(CH_3)_2C{=}NH{\bullet}H^+$ to form $(CH_3)_3C-NH_2{\bullet}^+$ must have an energy barrier associated with it, since the metastable ion decomposition of $(CH_3)_3C-NH_2{\bullet}^+$ displays a large kinetic energy release (11 kJ mol^{-1}) for alpha cleavage methyl radical loss. Although this energy barrier was not given by Hammerum and Derrick in their report, it has been demonstrated, using computational methods by Boyd, that methyl radical addition to imines exhibit activation energy barriers on the order of 27 kJ mol^{-1} [ΔH_{rxn} of -76 kJ mol^{-1} for $H_2C{=}NH\rightarrow(CH_3)H_2C{-}NH{\bullet}$] and 40 kJ mol^{-1} [$\Delta H_{rxn}$ of -62 kJ mol^{-1} for $(CH_3)HC{=}NCH_3\rightarrow(CH_3)_2HC{-}NCH_3{\bullet}$], respectively [38]. In the same report, computation results revealed that an activation energy barrier of 19 kJ mol^{-1} was associated with methyl radical addition to formaldehyde, [ΔH_{rxn} of -54 kJ mol^{-1} for $H_2C{=}O\rightarrow(CH_3)H_2C{-}O{\bullet}$] [38]. Denisov reported, in his review on free radical addition and activation energy, that methyl radical addition to acetone to form the tert-butoxy radical, exhibited an activation energy barrier of 56.5 kJ mol^{-1} [$(CH_3)_2C{=}O\rightarrow(CH_3)_3C{-}O{\bullet}$] [39].

Based on our data for the *m/z* 73 product ion and the literature results presented here, we hypothesize that $(CH_3)_3C-NH_2{\bullet}^+$, under our IMS–MS atmospheric chemical ionization conditions, is formed by methyl radical ($CH_3{\bullet}$) addition to the sp^2-hybridized carbon in 2-propanimine, $(CH_3)_2C{=}NH{\bullet}H^+$, surmounting an energy barrier on the order of 40 kJ mol^{-1}, which is likely facilitated by protonation of the nitrogen hetero-atom. Although this mechanism is highly speculative, evidence to support the production of methyl radicals has already been published: Oxley et al. [6] and Cotte-Rodriguez et al. [6,10]. demonstrated that thermal decomposition and fragmentation of TATP yields ethane, methane, methanol, 2-butanone and ethyl acetate dioxide by-products by way of methyl radical scavenging reactions taking place. Our experimental design has enabled us to chemically identify the *m/z* 73 product ion in the IMS or IMS–MS fragmentation spectra of TATP for the first time.

At this point, it is not clear how *m/z* 73 is actually being formed in the presence of IBA at low and high temperatures, but we speculate that it is feasible that it could be formed by either (1) IBA undergoing a proton assisted nucleophilic acyl substitution type reaction and releasing its $-NH_2$ group, which becomes protonated to form NH_3, NH_3 then reacts with TATP to form *m/z* 58, *m/z* 58 then undergoes rapid methyl radical attack to produce *m/z* 73, or (2) more likely from the presence of residual ammonia contamination in the IMS–MS system that reacts with TATP to initiate the chain of reactions that lead to the formation of *m/z* 73.

3.4.5. *m/z* 89 product ion peak

Similar to the *m/z* 73 product ion, an extensive literature search revealed that a proposed molecular formula has yet to be identified for the *m/z* 89 product ion that is associated with TATP (i.e. for its reduced mobility value that is observed in IMS). Under high temperature conditions when TATP is ionized in the presence of IBA, NH_3 and ND_3, the IMS–MS spectrum of TATP exhibits a high intensity peak for *m/z* 89, Fig. 3. At low temperatures, in the presence of the IBA additive, *m/z* 89 remained the most intense TATP product ion peak observed; however, in the presence of NH_3 and ND_3, the intensity of the *m/z* 89 product ion peak drastically decreased, with a significant increase in the intensity of the *m/z* 240 adduct peak, $TATP{\bullet}NH_4^+$, being observed, Fig. 3. These observations reveal that formation of *m/z* 89 is favored under the high temperature conditions and that the reaction pathway for its formation at low temperature is dictated by the adduct reagent used; specifically, coordination of NH_4^+ to TATP forms an adduct stable enough to hinder TATP from reacting further, thus obstructing the pathway for the formation of the *m/z* 89 product ion at low temperature. The binding energy of 25 kcal/mol for $TATP{\bullet}NH_4^+$ that was calculated by Sigman et al. [21]., relative to the calculated O–O bond energy of ~36 kcal/mol in TATP [6,7], provides a quantitative explanation for the stability of $TATP{\bullet}NH_4^+$. The *m/z* 89 product ion was also observed with moderate intensity in the ITMS–MS configuration; however, the *m/z* 58 product ion was the predominant peak observed under high and low temperature conditions in the presence of NH_3, Fig. 4. In the ITMS–MS spectrum, at low temperature with NH_3, a low intensity *m/z* 240 peak was also observed.

In the IMS–MS high temperature spectra of d_{18}-TATP, in the presence of IBA and NH_3, a deuterium shift from *m/z* 89 to *m/z* 98 is observed, Fig. 6. The corresponding deuterium mass shift is 9 amu, indicative of the *m/z* 98 product retaining three deuterated methyl groups [$(-CD_3)_3$ i.e. (C_3D_9)] from d_{18}-TATP, revealing that the original *m/z* 89 product ion contains a [C_3H_9] molecular component. In the IMS–MS ^{13}C-TATP spectrum, under high temperature conditions with both IBA and NH_3, the *m/z* 89 peak shifted by 1 amu to *m/z* 90, Fig. 7. The shift of 1 amu confirms that one of the ^{13}C-carbon atoms from the three ring carbons of TATP was present, producing an extended one carbon molecular component of [C_3H_9C]. To investigate the presence of nitrogen in the *m/z* 89 product ion, an IMS–MS spectrum of TATP was collected in the presence of $^{15}NH_3$. In this case, no shift of the product ion from *m/z* 89 to *m/z* 90 was observed, Fig. 5, indicating that the *m/z* 89 ion does not contain a nitrogen atom. When TATP was ionized in the presence of ND_3, it was observed that the single *m/z* 89 product ion peak did not split into multiple peaks, Fig. 5, verifying that this product ion does not contain multiple hydrogen atoms that are capable of undergoing hydrogen–deuterium exchange. As stated earlier, we attribute the minor intensity shoulder peaks associated with *m/z* 89 to a ^{13}C-natural abundance contribution (i.e. *m/z* 90) and to the direct formation of an additional TATP product ion (i.e. *m/z* 91), both of which have been previously observed [19–22,25,33]. The *m/z* 91product ion has been

postulated as having the molecular formula of $C_3H_6O_3 \bullet H^+$ [19,20,25,33].

MS–MS analysis of the *m/z* 89 and deuterated *m/z* 98 product ions produced single daughter ion peaks at *m/z* 43 and *m/z* 46, respectively. The *m/z* 46 daughter ion peak exhibits the expected isotopic peak shift of 3 amu, representative of a (CH_3) group being present in the original *m/z* 43 daughter ion (i.e. in the corresponding *m/z* 89 product ion). MS–MS analysis of the ^{13}C-labeled *m/z* 90 product ion produced a daughter ion peak at *m/z* 44, yielding the expected 1 amu isotopic shift from the *m/z* 43 peak, confirming that *m/z* 43 contains one of the ring carbons from TATP. As stated above, the *m/z* 89 does not contain any nitrogen atoms and does not contain any hydrogen atoms that are capable of undergoing hydrogen–deuterium exchange. Based on these results, we conclude that the *m/z* 43 daughter ion produced from *m/z* 89 is identical to the previously proposed formula of $(CH_3)CO^+$, yielding the corresponding deuterated isotopologue $(CD_3)CO^+$ (*m/z* 46) [20,21,24,25,34]. Taking the presence of oxygen into account, the component of *m/z* 89 described heretofore, [C_3H_9C], can be extended by one oxygen atom to [C_3H_9CO]. The calculated molecular weight for [C_3H_9CO] is 73, a mass difference of 16 from *m/z* 89 parent ion. Since the chemical regents used in this study were TATP [i.e. $(CH_3)_6C_3O_6$], IBA [i.e. $(CH_3)_2CHCONH_2$] and NH_3, the remaining elemental components that can come from these reagents that satisfy the mass difference of 16 are $-O$, $-NH_2$, and CH_4. The $-NH_2$ component can be ruled out because as demonstrated through this work with ND_3, the *m/z* 89 does not contain any nitrogen atoms (or hydrogen atoms readily capable of undergoing hydrogen–deuterium exchange). Therefore, *m/z* 89 may be composed of one of two possible molecular formulas, [$(CH_3)_3CO_2^+$] or [$(CH_3)_3COCH_3 \bullet H^+$]. As revealed above, the d_{18}-TATP spectra of Fig. 6 exhibited a deuterium shift from *m/z* 89 of 9 amu, which suggests that the *m/z* 89 contains three methyl groups [$(-CH_3)_3$] and not four [$(-CH_3)_4$]. If *m/z* 89 contained four methyl groups from d_{18}-TATP, a corresponding deuterium shift of 12 amu would have been observed. Based on the result that *m/z* 89 is produced as the major intensity product ion of TATP in the presence of IBA as well as NH_3 at high temperature (Figs. 3, 6 and 7), we conclude that it is unlikely that a CH_3 group is coming from the presence or break down of the additive reagents. Thus, we rule out [$(CH_3)_3COCH_3 \bullet H^+$] as a possibility and suggest *m/z* 89 as having the molecular formula of [$(CH_3)_3CO_2^+$].

As stated above, *m/z* 58 is a minor product ion observed in IMS–MS that is produced only in the presence of NH_3 at low and high temperatures and has been proposed to form from TATP by way of an ammonia driven (C–O bond cleavage initiated) reaction pathway, Figs. 3 and 8. In contrast, the *m/z* 89 product ion forms as the major product ion from TATP in the presence of NH_3 at high temperature and in the presence of IBA under both low and high temperature conditions in the IMS–MS, Fig. 3, indicating that *m/z* 89 is forming by way of a different reaction pathway. It is worth reiterating that the *m/z* 240 (TATP$\bullet NH_4^+$) and *m/z* 310 (TATP-IBA$\bullet H^+$) adducts are not observed at high temperature and that TATP$\bullet NH_4^+$ is observed as the major product ion only at low temperature in the presence of NH_3, Fig. 3; these results suggest, in regard to the formation of *m/z* 89 as the primary product ion, that TATP reacts before it has a chance to complex with NH_4^+ or IBA at high temperature, or that TATP$\bullet NH_4^+$ and TATP-IBA$\bullet H^+$ ions are not stable at high temperature and rapidly undergo further reaction. Previous work by Oxley et al. [6]. revealed that thermal decomposition of TATP, in the absence of an additive reagent, at 151 °C to 230 °C is a first-order reaction that yields acetone (about 2 mole per mole of TATP) as the principle decomposition product, exhibiting an Arrhenius dependence on temperature with an activation energy of 36.3 kcal/mol and a pre-exponential constant of $3.75 \times 10^{13}\ s^{-1}$; based on these experimental results, Oxley et al. proposed that the first step in the gas phase thermal decomposition of TATP between 151 °C and 230 °C involved O–O bond cleavage. Similarly, based on theoretical results, Dubnikova et al. [7]. proposed that the thermal decomposition of TATP involved an initial O–O bond cleavage step, with a calculated activation energy of ~36 kcal/mol, a pre-exponential constant of $\sim 5.7 \times 10^{16}\ s^{-1}$ and the loss of two moles of acetone.

We propose that after an initial O–O bond cleavage step followed by the loss of two moles of acetone, the *m/z* 89 is formed by methyl radical attack on a carbonyl oxide intermediate, followed by one electron oxidation of the tert-butyl radical species by way of collision with an oxidizing agent, Fig. 9. Evidence for the production of methyl radical scavengers during TATP thermal decomposition has been established by Oxley et al. [6]. and Cotte-Rodriguez et al. [6,10]. The experimental and theoretical work described in the reviews by Sander [40] and Bunelle [41] demonstrate that carbonyl oxide ($C_3H_6O_2$) is a short-lived and highly reactive intermediate that is best viewed as a diradical in equilibrium with its zwitterionic state, with the isomeric form, dioxirane, lying at the lowest energy state of all three isomeric forms. Specifically, using electronic structure calculations employing the cc-pVDZ basis set at the DFT B3LYP level of theory, Dubnikova et al. demonstrated that the thermal decomposition pathway of TATP, following the initial O–O bond cleavage step,

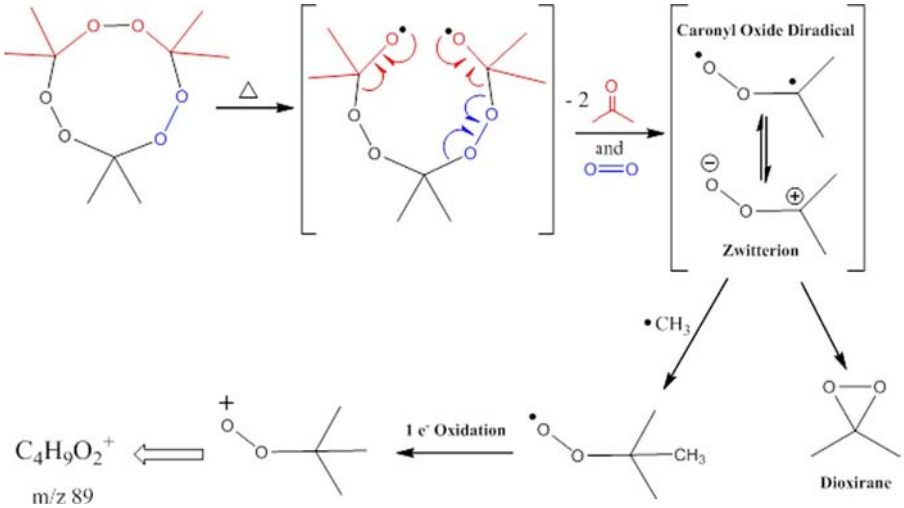

Fig. 9. Proposed reaction scheme for the formation of the *m/z* 89 product ion.

does in fact involve production of the highly reactive carbonyl oxide intermediate, with his calculations also revealing that dioxirane sits at the lowest energy level of the isomeric forms [7]. Based on our data and the literature results presented here, a molecular formula, $[(CH_3)_3CO_2^+]$, for *m/z* 89 and a reaction pathway for its formation has been proposed, Fig. 9.

4. Conclusion

The identity and molecular formulas of several of the major product ions of TATP have not been well characterized in the literature, and in some cases, even the chemical identity of some product ions has not yet been postulated. IMS-based detection of TATP product ions is primarily achieved wherein ions produced in the IMS reaction region are mainly identified by their drift time (i.e. mobility value or specific peak positions in the mobility spectrum), as compared to algorithmic libraries based on empirical data, employing limited knowledge of the ion chemistry taking place. In general, identifying product ions in IMS systems primarily based on peak position often can lead to false detection (i.e. false alarms). In order to help resolve such issues, two recently developed COTS IMS instruments were coupled to triple–quadrupole mass spectrometers and isotopic labeling experiments of TATP were performed. The integrated IMS–MS and ITMS–MS systems have been employed in this study, along with the dopants IBA and ammonia, to obtain mobility spectra and corresponding *m/z* ratios for each product ion of TATP produced. Following mass determinations, isotope labeling experiments were conducted and the isotopic shift results were used to verify the identity and molecular formulas of previously identified *m/z* 58 and 240 TATP product ions. Mass determinations and isotope labeling experiments were also conducted to help identify and predict molecular formulas for previously incompletely characterized *m/z* 73 and 89 TATP product ions. This work postulated the mechanism of formation for the product ions of TATP and proposed the identity of the *m/z* 58, 73, 89 and 240 product ions to be $[(CH_3)_2C{=}NH{\bullet}H^+]$, $[(CH_3)_3C-NH_2{\bullet}^+]$, $[(CH_3)_3CO_2^+]$ and $[TATP{\bullet}NH_4^+]$, respectively. It is anticipated that this work will not only help to facilitate improvements in current IMS-based detection, but also will aid in the development and optimization of other atmospheric ionization detection technologies, particularly mass spectrometry-based equipment.

Acknowledgments

The research was supported in part by the US Department of Homeland Security Science and Technology Directorate. This research was supported in part by an appointment for Dr. Tomlinson-Phillips to the Transportation Security Laboratory Visiting Scientist Program administered by the Oak Ridge Institute for Science and Education (ORISE) through an interagency agreement between the US Department of Energy (DOE) and the US Department of Homeland Security. ORISE is managed by Oak Ridge Associated Universities (ORAU) under DOE Contract no. DE-AC05-06OR23100. The US Department of Homeland Security Science and Technology Directorate, Transportation Security Laboratory sponsored this work under an interagency agreement with ORISE, no. HSHQDC-06-X-00329. Dr. Kozole was funded through an interagency agreement between the US Department of Homeland Security Science and Technology Directorate, Transportation Security Laboratory and the Naval Research Laboratory under IAA no. HSHQDC-10-X-00444.

Appendix A. Supporting information

Supplementary data associated with this article can be found in the online version at http://dx.doi.org/10.1016/j.talanta.2014.03.044.

References

[1] H.W.S. Ostmark, H.G. Ang, Propellants Explos. Pyrotech. 37 (2012) 12–23.
[2] D.S. Moore, Rev. Sci. Instrum. 75 (2004) 2499–2512.
[3] D.S. Moore, Sens. Imaging 8 (2007) 9–38.
[4] R. Wolffenstein, Ber. der Dtsch. Chem. Ges. 28 (1895) 2265–2269.
[5] N.A. Milas, A. Golubovic, J. Am. Chem. Soc. 81 (1959) 6461–6462.
[6] J.C. Oxley, J.L. Smith, H. Chen, Propellants Explos. Pyrotech. 27 (2002) 209–216.
[7] F.K.R Dubnikova, J. Almog, Y. Zeiri, R. Boese, H. Itzhaky, A. Alt, E. Keinan, J. Am. Chem. Soc. 127 (2005) 1146–1159.
[8] C. Mullen, D. Huestis, M. Coggiola, H. Oser, Int. J. Mass Spectrom. 252 (2006) 69–72.
[9] I. Cotte-Rodríguez, H. Chen, R.G. Cooks, Chem. Commun. (2006) 953.
[10] I. Cotte-Rodrıguez, H. Hernandez-Soto, H. Chen, R.G. Cooks, Anal. Chem. 80 (2008) 1512–1519.
[11] K. Yeager, R.L. Woodfin (Eds.), John Wiley & Sons, Hoboken, NJ, 2007.
[12] R. Schulte-Ladbeck, M. Vogel, U. Karst, Anal. Bioanal. Chem. 386 (2006) 559–565.
[13] G.W. Cook, P.T. LaPuma, G.L. Hook, B.A. Eckenrode, J. Forensic Sci. 55 (2010) 1582–1591.
[14] G.A. Eiceman, E.V. Krylov, E.G. Nazarov, R.A. Miller, Anal. Chem. 76 (2004) 4937–4944.
[15] D.D. Fetterolf, T.D. Clark, J. Forensic Sci. 38 (1993) 28–39.
[16] R.G.A. Ewing, D.A., G.A. Eiceman, G.J. Ewing, Talanta 54 (2001) 515–529.
[17] I., Cho; T., Chamberlain; S., Brunk; R., Gill; D., LaMonica in: Proceedings of the 3rd International Aviation Security Technology Symposium Atlantic City, NJ, 2001, pp. 1–13.
[18] A.J., Marr; D.M., Groves in: Proceedings of the International Society for Ion Mobility Spectrometry, 2003; vol. 6, pp. 59–62.
[19] R.G. Ewing, M.J. Waltman, D.A. Atkinson, Anal. Chem. 83 (2011) 4838–4844.
[20] C. Shen, J. Li, H. Han, H. Wang, H. Jiang, Y. Chu, Int. J. Mass Spectrom. 285 (2009) 100–103.
[21] M.E. Sigman, C.D. Clark, R. Fidler, C.L. Geiger, C.A. Clausen, Rapid Communications in Mass Spectrometry 20 (2006) 2851–2857.
[22] L. Widmer, S. Watson, K. Schlatter, A. Crowson, Analyst 127 (2002) 1627–1632.
[23] X. Xu, A.M.V.D. Craats, E.M. Kok, P.C.A.M.D. Bruyn, J. Forensic Sci. 49 (2004) 1–7.
[24] A.J. Peña-Quevedo, R. Cody, N. Mina-Camilde, M. Ramos, S.P. Hernández-Rivera, Proc. SPIE 6538 (2007) 653828.
[25] P.F. Wilson, B.J. Prince, M.J. McEwan, Anal. Chem. 78 (2006) 575–579.
[26] J. Kozole, J.R. Stairs, I. Cho, J.D. Harper, S.R. Lukow, R.T. Lareau, R. DeBono, F. Kuja, Anal. Chem. 83 (2011) 8596–8603.
[27] J.T.-P.J. Kozole, J.R. Stairs, J.D. Harper, S.R. Lukow, R.T. Lareau, H. Boudries, H. Lai, C.S. Brauer, Talanta 99 (2012) 799–810.
[28] Yinon, J. in: Proceedings of the International Symposium on the Analysis and Detection of Explosives Quantico, Virginia, 1983, pp. 227–234.
[29] C.S., Brauer; J., Barber; J.C., Weatherall; B.T., Smith; J., Tomlinson-Phillips; A., Wooten in: E. M. Carapezza (Ed.), Proceedings of SPIE: Sensors, and Command, Control, Communications, and Intelligence Technologies for Homeland Security and Homeland Defense, 2011; vol. 8019.
[30] M.A. Walter, D. Pfeifer, W. Kraus, F. Emmerling, R.J. Schneider, U. Panne, M.G. Weller, Langmuir: ACS J. Surf. Colloids 26 (2010) 15418–15423.
[31] G. Buttigieg, Forensic Sci. Int. 135 (2003) 53–59.
[32] G.A. Eiceman, Z. Karpas, Ion Mobility Spectrometry, second ed., CRC Press Taylor & Francis Group, Boca Raton, FL, 2005.
[33] S., Zitrin; S., Kraus; B., Glattstein in: Proceedings of the International Symposium on the Analysis and Detection of Explosives FBI Academy, Quantico, Virginia, 1983.
[34] R. Rasanen, M. Nousiainen, K. Perakorpi, M. Sillanpaa, L. Polari, O. Anttalainen, M. Utriainen, Anal. Chim. Acta 623 (2008) 59–65.
[35] M. Schmittel, A. Burghart, Angew. Chem. Int. Ed. Engl. 36 (1997) 2550–2589.
[36] R.L. McCormick, J.R. Baker, H.W., J. Haynes, R. Malhotra, Enegy Fuels 2 (1988) 740–743.
[37] S. Hammerum, P.J. Derrick, J. Chem. Soc. Chem. Commun. (1985) 996.
[38] S.L. Boyd, R.J. Boyd, J. Phys. Chem. A 105 (2001) 7096–7105.
[39] E.T. Denisov, Russ. Chem. Rev. 69 (2000) 153–164.
[40] W. Sander, Angew. Chem. Int. Ed. Engl. 29 (1990) 344–354.
[41] W.H. Bunnelle, Chem. Rev. 91 (1991) 335–362.